A Letters Journal Exploring the Frontiers of Physics

January 2008

EPL, **81** (2008) 24001
doi: 10.1209/0295-5075/81/24001

www.epljournal.org

Burst avalanches and inter-occurrence times in creep rupture

Th. Baxevanis[1] and Th. Katsaounis[1,2]

[1] *Department of Applied Mathematics, University of Crete - Heraklion 714 09, Greece*
[2] *IACM, FORTH - Heraklion 711 10, Greece*

received 29 June 2007; accepted in final form 8 November 2007
published online 4 December 2007

PACS 46.35.+z – Viscoelasticity, plasticity, viscoplasticity
PACS 46.50.+a – Fracture mechanics, fatigue and cracks
PACS 62.20.Mk – Fatigue, brittleness, fracture, and cracks

Abstract – The statistics of fracture precursors in the creep-damage process are studied on the basis of a proposed dry, non-linear viscoelastic fiber bundle model. This model permits the occurrence of damage avalanches consisting of simultaneous rupture of several fibers. The avalanche size distribution for the *global-load sharing* rule follows a power law asymptotic behavior analogous to that of static fracture (Kloster M. *et al.*, *Phys. Rev. E*, **56** (1997) 2615). The statistical behavior of the same distribution, however, for the *local-load sharing* rule is different from that of the static fracture. Moreover, power law asymptotics apply to times between successive bursts with a *universal* exponent close to unity —an exponent close to that observed in fracturing processses occuring at vastly different time and space scales.

Introduction. – Statistical aspects of rupture in random materials have received increasing attention due to their richness in physical and mathematical phenomena. It is still, however, an open problem to embed material fracture into the general framework of statistical physics. Among the fundamental problems that statistical physics face is to understand the analogy of material failure with thermodynamic phase transitions and critical phenomena [1]. This field has attracted the attention of physicists due to the existence of power laws and fractals expressing the self-organization of the rupture process. The acoustic emission (AE) recorded in stressed materials under constant stress or constant strain rate loading exhibits a wealth of such "critical" behaviors. In particular, the temporal, spatial and size distributions of the acoustic emission (AE) events follow a power-law-like statistics [2,3]. Such a power law scaling is observed also in earthquakes [4,5], despite the vastly different scales involved, and can be considered indicative of self-similarity in the AE and earthquake source process [6]. AE is the consequence of micro-cracks forming and propagating in the material and thus provide an indirect measure of the damage accumulated in the system. For this reason, AE is often used as a non-destructive tool in material testing and evaluation.

Conceptually simple models are an attractive tool for the needs of the statistical-physics approach. While simple models often fail to reproduce the complex phenomenology observed, they can nevertheless provide meaningful insights. Moreover, qualitative features of such models may be amenable to experimental testing [7,8]. The earliest and simplest models in this respect are the fiber bundle models (FBMs) [9]. In the case of fast fracture, the classic work is that of Daniels [10] while in the case of time-dependent breakdown the seminal work is that of Coleman's [11]. Recently, creep observations have been modeled in terms of novel FBMs with viscoelastic fibers [7, 12,13]. These models, however, do not embody the classical static feature of instant multiple cracks; they resemble the classical time-dependent FBMs in this respect. In the static case burst avalanches occur as load redistribution following fiber failures may cause step load increases on surviving fibers above their stress threshold. In the time-dependent models, failure probability, controlled by lifetime (in the classical time-dependent FBMs) or strain thresholds (in the viscoelastic FBMs), remains continuous under these step increases in fiber load; fibers break one by one. This is not the case however for the time-dependent FBMs with thermal noise also proposed for the study of the creep behavior of disorder systems [8,14], in which instant multiple fiber breaks are possible. Although the avalanche size distribution is not related directly to any fracture experiments, it has been proved of outmost importance in the theoretical description of the fracturing process [15].

In [16], the viscoelastic FBMs of [12] were enriched by a more realistic rheology in order to account for burst avalanches of simultaneous fiber breaks. The rheology of

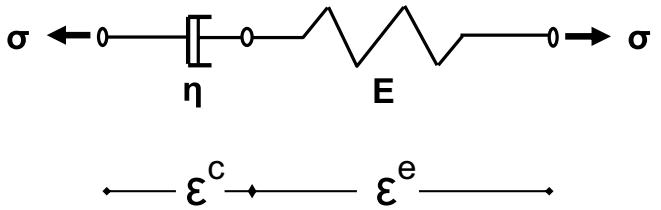

Fig. 1: The proposed Maxwell rheological model describing the constitutive behavior of the bonds.

the fibers in this work is described by the Kelvin-Voigt chain model which is amenable to approximate any *linear* viscoelastic material to any desired accuracy. This model provides an adequate approach for the statistical analysis of fracture precursors in the creep rupture of natural fiber composites like wood [17]. Here, we extend this analysis using *non-linear* viscoelastic rheology for the fibers. Such an FBM is more appropriate for fiber-reinforced composites. Namely, the avalanche size and inter-event time distribution (the inter-event times distribution is affected on average by the avalanche size distribution) are analyzed for the two ends of the load redistribution spectrum, *i.e.* for global and local load sharing rules. The results obtained, especially that on the temporal occurence of fracturing events, are considered of importance in non-destructive testing and earthquake prediction.

Non-linear viscoelastic fiber bundle model. – The model consists of a 1D linear array of N fibers, pulled parallel to their direction by an external load. The fibers are assumed to exhibit *non-linear* viscoelasticity described by the Maxwell equation

$$\dot{\varepsilon}^t(t) = \frac{\dot{\sigma}(t)}{E} + \frac{\sigma^m(t)}{\eta}, \tag{1}$$

where $\sigma(t)$ is the applied stress, $\varepsilon^t(t)$ the corresponding strain, E Young's modulus and η, $m \geqslant 1$ the creep constant and creep exponent, respectively. This constitutive equation has considerable validity for the description of the steady-state creep of single-phase metals and ceramics for both elevated temperatures and high applied stresses [18]. Typical values of m for such materials range between 3 and 6. The m exponent is a measure of the non-linearity of the material response; for $m = 1$ the response is linear viscoelastic. Equation (1) resembles a Maxwell element which consists of a spring and a dashpot coupled in series as illustrated in fig. 1, thus it actually decouples to the system

$$\begin{cases} \varepsilon^t(t) = \varepsilon^e(t) + \varepsilon^c(t), \\ \sigma(t) = E\varepsilon^e(t), \\ \sigma^m(t) = \eta\dot{\varepsilon}^c(t), \end{cases} \tag{2}$$

where ε^e and ε^c are the parts of the strain that correspond to the deformation of the spring and dashpot, respectively. In order to capture failure in the model a strain-controlled failure criterion is imposed, *i.e.* a fiber fails during the time evolution of the system when its total strain exceeds a statistically distributed damage threshold ε^d with probability density $p(\varepsilon^d)$ and cumulative distribution $P(\varepsilon^d) = \int_0^{\varepsilon^d} p(x)\mathrm{d}x$.

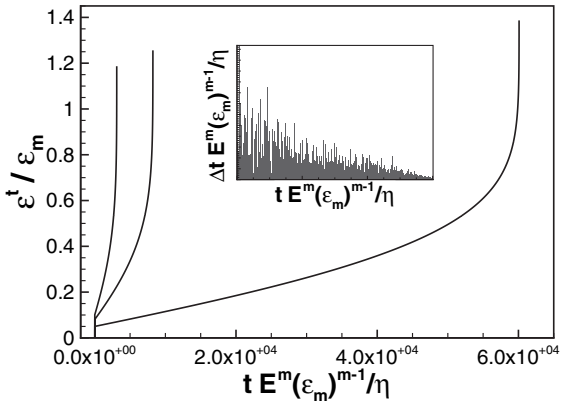

Fig. 2: Total strain $\varepsilon^t(t)$ for several values of σ_0 with a creep exponent $m = 4$ (Weibull distribution $P(\varepsilon^d) = 1 - \exp[-(\varepsilon^d/\varepsilon_m)^\alpha]$, $\alpha = 2$). The inset represents typical values of times Δt between successive bursts. The figure is based on bundles of $N = 10^7$ fibers.

The simplest approach is to assume the global load sharing rule (GLS), *i.e.* after failure of a fiber its load is transfered equally among the intact fibers, so that the load on fiber i at a certain deformation ε^t is simply given by $\sigma_i(\varepsilon^t) = \sigma(\varepsilon^t)/n_s(\varepsilon^t) = \sigma(\varepsilon^t)/[N(1 - P(\varepsilon^t)]$, where $n_s(\varepsilon^t)$ is the total number of surviving fibers. Thus the macroscopic constitutive equation for the time evolution of the bundle is described by the system

$$\begin{cases} \varepsilon^t = \varepsilon^e + \varepsilon^c, \\ \sigma = [1 - P(\varepsilon^t)]E\varepsilon^e, \\ \sigma^m = [1 - P(\varepsilon^t)]^m\eta\dot{\varepsilon}^c. \end{cases} \tag{3}$$

We restrict our attention to loading paths in which the stress remains fixed to a constant value σ_0. The creep rupture displacement $\varepsilon_r^t = \varepsilon_r^e + \varepsilon_r^c$ —the total strain at the time t_f of complete rupture— corresponds to the values of ε^e and ε^c that satisfy $\sigma_0 = [1 - P(\varepsilon^e + \varepsilon^c)]E\varepsilon^e = \phi(\varepsilon^e, \varepsilon^c)$ and vanish $\partial\phi/\partial\varepsilon^e = 1 - P(\varepsilon^t) - \varepsilon^e p(\varepsilon^t)$. Indeed, $\mathrm{d}\sigma_0 = (\partial\phi/\partial\varepsilon^e)\mathrm{d}\varepsilon^e + (\partial\phi/\partial\varepsilon^c)\mathrm{d}\varepsilon^c = 0$ yields $\dot{\varepsilon}^e \to \infty$ for $\partial\phi/\partial\varepsilon^e \to 0$. Creep rupture occurs eventually for all loads; there is no critical stress. However, for very small values of the applied load the complete rupture does not occur in a time scale of interest. In fig. 2, the behavior of ε^t is illustrated for different values of the applied stress. Note that the bundle displays no primary creep (or logarithmic creep), *i.e.* after the initial elastic response the creep rate does not slowly decrease with increasing strain but it practically jumps to a nearly constant value that depends on the value of the applied load (steady-state creep). This behavior is attributed on the constitutive equation (1) that describes only the steady-creep stage.

Burst avalanches. Creep is a stress-controlled process, thus the same load must always be endured by the

surviving fibers; the same load is simply redistributed. Step load increases following fiber failure —the stresses are assumed to equilibrate infinitely fast (quasistatic assumption)— result in instantaneous increases in elastic strain due to the presence of the elastic unit in the Maxwell element (fig. 1). Therefore it is likely that the (total) strain threshold of other non-failed fibers may be exceeded. This mechanism may easily trigger an avalanche. It should be noted that the dynamics of avalanches of fiber breaks is different for the static and the proposed viscoelastic model. Whenever an avalanche stops in the static model, the load of each of the surviving fibers increases so as to become equal to the next stress threshold and then a new avalanche may occur due to the failure of the fiber having this threshold as its strength. In the proposed model however, whenever an avalanche stops, the load of the fibers remains constant until the creep (time-dependent) deformation forces the total deformation to reach the next threshold.

In order to derive analytically the distribution $D(\Delta)$ of bursts Δ for GLS, consider a small strain per fiber interval $(\varepsilon^t, \varepsilon^t + \mathrm{d}\varepsilon^t)$. For a large number N of fibers the expected number of surviving fibers in this interval is $N[1-P(\varepsilon^t)]$. Moreover, the expected number of thresholds in the interval is $Np(\varepsilon^t)\mathrm{d}\varepsilon^t$. These thresholds are Poisson distributed. Assume that time-dependent deformation results in the break of a fiber with threshold ε^t, then the load that this fiber suffered will be redistributed on the $N[1-P(\varepsilon^t)]$ remaining fibers; the average force σ_0 remains fixed. Thus the instantaneous load increase will be $\mathrm{d}\sigma = E\varepsilon^e/\{N[1-P(\varepsilon^t)]\}$ which results in a total strain increase $\mathrm{d}\varepsilon^t = \mathrm{d}\varepsilon^e = \varepsilon^e/\{N[1-P(\varepsilon^t)]\}$, since the creep strain remains fixed. The average number of fibers that break due to this load increase is

$$\alpha = \alpha(\varepsilon^t) = Np(\varepsilon^t)\mathrm{d}\varepsilon^t = \frac{\varepsilon^e p(\varepsilon^t)}{[1-P(\varepsilon^t)]}. \tag{4}$$

Following the analysis in [19,20], one finds that the distribution of bursts Δ over an interval $(\varepsilon_0^t, \varepsilon_r^t)$ is given by

$$\frac{D(\Delta)}{N} = \frac{\Delta^{\Delta-1}}{\Delta!}\int_{\varepsilon_0^t}^{\varepsilon_r^t} \alpha(\varepsilon^t)^{\Delta-1} e^{-\alpha(\varepsilon^t)\Delta}[1-\alpha(\varepsilon^t)]p(\varepsilon^t)\mathrm{d}\varepsilon^t. \tag{5}$$

For large Δ the maximum contribution comes from the neighborhood of the upper integration limit, since $\alpha(\varepsilon^t)e^{-\alpha(\varepsilon^t)}$ is maximal for $\alpha(\varepsilon^t)=1$, *i.e.* for $\varepsilon^t = \varepsilon_r^t$. Expansion around the saddle point using $\alpha^\Delta e^{-\alpha\Delta} = e^{\Delta[-1-1/2(1-\alpha)^2+\mathcal{O}(1-\alpha)^3]}$, as well as $\alpha(\varepsilon^t) \backsimeq 1 + \alpha'(\varepsilon_r^t)(\varepsilon^t - \varepsilon_r^t)$ and Stirling's approximation $\Delta! = \Delta^\Delta e^{-\Delta}\sqrt{2\pi\Delta}$, one obtains

$$\frac{D(\Delta)}{N} = C\Delta^{-5/2}(1-e^{-\Delta/\Delta_c}), \tag{6}$$

where

$$\Delta_c = 2/[\alpha'(\varepsilon_r^t)^2(\varepsilon_r^t - \varepsilon_0^t)^2] \tag{7}$$

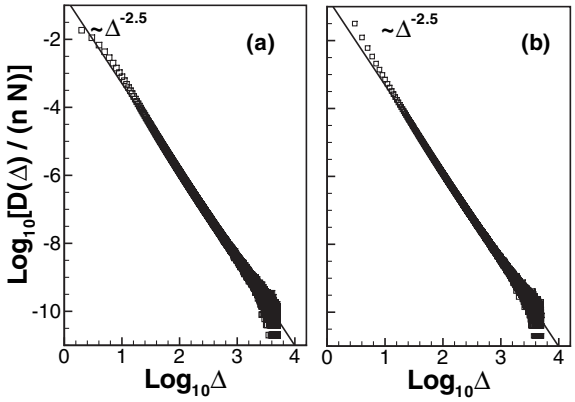

Fig. 3: (a) A log-log plot of the distribution of bursts for GLS recorded in the interval $(0, \varepsilon_r^t)$ ($m=6$, uniform distribution $P(\varepsilon^d) = \varepsilon^d/\varepsilon_m$). (b) A log-log plot of the distribution of bursts for GLS recorded in the interval $(0, \varepsilon_r^t)$ ($m=5$, Weibull distribution $\alpha=3$). Both figures are based on $n = 5\cdot 10^4$ bundles of $N = 10^6$ fibers.

and $C = (2\pi)^{-1/2}p(\varepsilon_r^t)/\alpha'(\varepsilon_r^t)$. Equation (6) yields the asymptotic behavior

$$\frac{D(\Delta)}{N} \propto \begin{cases} \Delta^{-3/2}, & \text{for} \quad \Delta \ll \Delta_c, \\ \Delta^{-5/2}, & \text{for} \quad \Delta \gg \Delta_c. \end{cases} \tag{8}$$

Such a behavior has been proved in the static [19] and linear viscoelastic [17] global FBMs. This behavior is a universal phenomenon, independent of the threshold distribution, the applied stress and the creep exponent (fig. 3). The crossover has been proposed as a signal for imminent failure [20]; the 3/2 power law will be seen only when the beginning of the interval, ε_0^t, is close enough to the rupture value ε_r^t. Hence, for applications it is important that the crossover signals are seen also in a single sample (fig. 4a). In addition, the exact value of the crossover point has been derived (7). For the uniform distribution $\Delta_c = 2(1-\varepsilon_r^t)/[(\varepsilon_r^t)^2(1-\varepsilon_0^t/\varepsilon_r^t)^2]$ (dimensionless values) where $\varepsilon_r^t = 1-\sqrt{\sigma_0}$, so for $\sigma_0 = 0.2$ and $\varepsilon_0^t = 0.6\varepsilon_r^t$ one obtains $\log(\Delta_c) \simeq 1.26$. This value is approximated reasonably well by numerical simulations (fig. 4b). For the other extreme case of load sharing that the local-load sharing rule (LLS) constitutes, in which the excess load of a bursting fiber is divided equally to the nearest surviving fibers, the numerically estimated apparent exponent value for small event sizes is *not* universal but dependent on the microstructural details (the threshold distribution) (fig. 5). Moreover, for different applied stresses the exponent may vary considerably (fig. 5). The trend is that the smaller the applied load is the smaller the absolute value of the exponent. This behavior is in contrast to the static and linear viscoelastic FBMs in which the exponent is approximated quite well by the value -4.5 (for small event sizes).

Inter-event times. Next, we study numerically the distribution $D(\Delta t)$ of times Δt in between successive

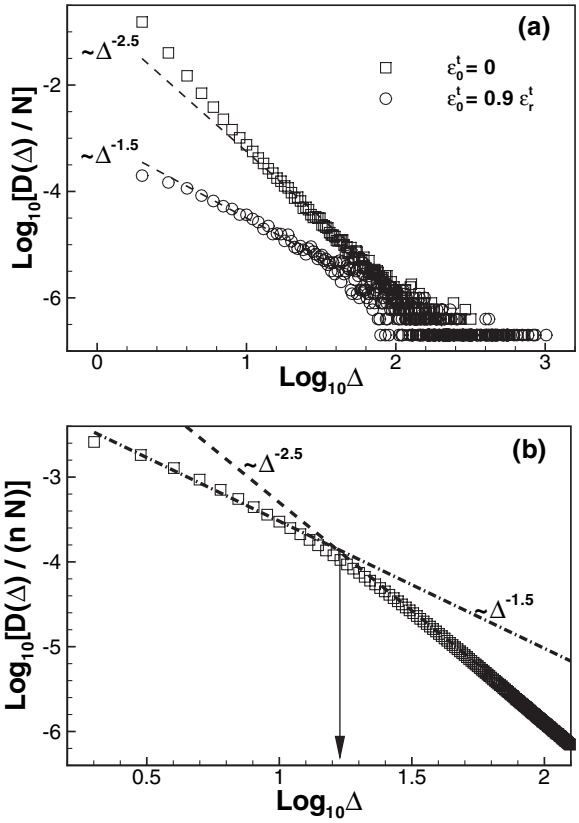

Fig. 4: (a) A log-log plot of the distribution of bursts under GLS recorded in an interval $(\varepsilon_0^t, \varepsilon_r^t)$. The creep exponent and Weibull exponent are $m = 7$ and $\alpha = 3$, respectively. The figure is based on a bundle of $N = 10^7$ fibers. (b) The distribution of bursts for the uniform threshold distribution with $\sigma_0/(E\varepsilon_m) = 0.02$ and $\varepsilon_0^t = 0.6\varepsilon_r^t$ $(m = 3)$. The figure is based on $n = 5 \cdot 10^4$ bundles of $N = 10^6$ fibers. The arrow indicates the crossover point.

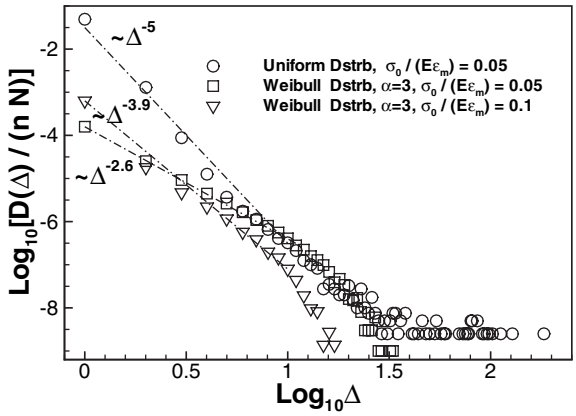

Fig. 5: A log-log plot of the distribution of bursts under LLS recorded in an interval $(0, \varepsilon_r^t)$. The applied loads and threshold distribution are described in the legend $(m = 6)$. The figure is based on $n = 10^4$ bundles, each with $N = 10^5$ fibers.

bursts. The inter-event times between successive bursts for the proposed model depend on the applied load, the applied probability distribution and the creep exponent.

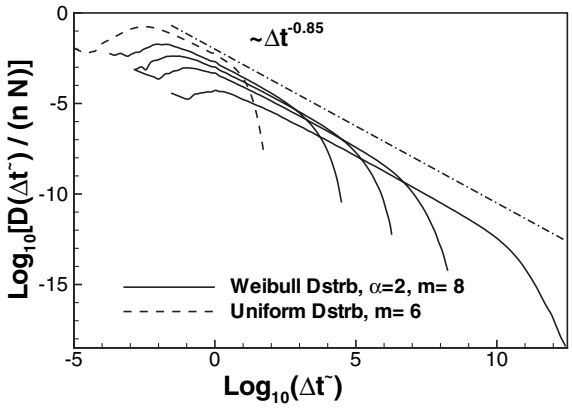

Fig. 6: A log-log plot of the distribution of inter-event times $\Delta t^{\tilde{}}$ $(t^{\tilde{}} = tE^m(\varepsilon_m)^{m-1}/\eta)$ under GLS for several values of applied stress. The γ-value remains the same for different stresses, threshold distribution and creep exponent. The power law behavior can be observed over 5 orders of magnitude. The figure is based on $n = 1000$ samples of $N = 10^7$ fibers.

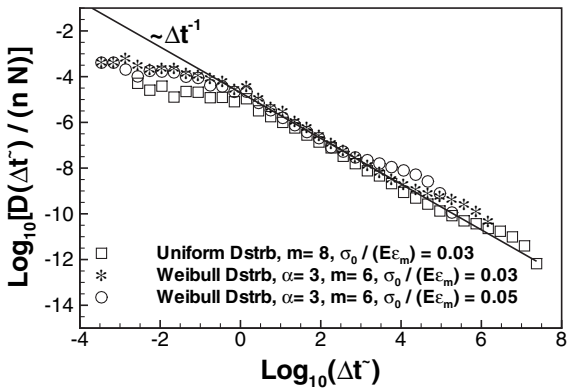

Fig. 7: A log-log plot of the distribution of inter-event times $\Delta t^{\tilde{}}$ $(t^{\tilde{}} = tE^m(\varepsilon_m)^{m-1}/\eta)$ for LLS. The γ-value remains the same for different stresses, threshold distribution and creep exponent. The figure is based on $n = 1000$ samples, each with $N = 10^5$ fibers.

However, a universal feature is that the peaks of Δt initially, along the steady-creep stage, are scattered over a broad interval while they decay more or less exponentially in the tertiary stage (fig. 2). Moreover, extensive simulations under GLS revealed that the distribution of inter-event times on the macroscopic steady-creep stage follows a power law of the form $D(\Delta t) \propto \Delta t^{-\gamma}$. The value of the exponent $\gamma = 1 \pm 0.05$ is independent from the disorder distribution, the applied load and the creep exponent (fig. 6). Note that increasing the load or decreasing the creep exponent m, the power law regime preceding the exponential cut-off is getting shorter but the value of γ remains the same. A similar exponential decay of the statistical distribution of inter-event times with an exponent $\gamma = 1 \pm 0.05$ was found under LLS, as well, independent again from the applied load, failure distribution and creep exponent (fig. 7). These results are in agreement

with those from viscoelastic FBMs [17]. The empirical value of the exponent γ obtained from experiments was found to depend on the material. Nevertheless, the values reported in literature are in the proximity of unity [2] with the exception of [3].

The differences between our theoretical results and those in [13,21] on the γ-value are worth mentioning. In contrast to our results, in [13], the exponent γ is not universal; it is different for GLS on the two sides of the critical stress σ_c ($\gamma \simeq 1.5$ for $\sigma_0 > \sigma_c$ and $\gamma \simeq 1.95$ for $\sigma_0 < \sigma_c$, these values were also obtained from a completely different approach of creep failure [21]), while for LLS the system is in the same universality class ($\gamma \simeq 1.9$) as for GLS for stress levels above the critical one. The discrepancy between the latter results and those reported herein are attributed to the influence on inter-event times distributions by the burst avalanches present in our model; in [13,21] fibers break one by one.

Conclusions. – Concluding, a dry FBM of non-linear viscoelastic fibers is proposed for the study of fracture precursors in creep rupture. The constitutive behavior of the fibers resembles a Maxwell unit amenable to approximate the rheology of single-phase metals and ceramics for both elevated temperatures and high applied stresses. In particular, the event sizes and event time intervals follow a power-law-like statistics. The power law asymptotic behavior of event sizes for GLS is analogous to that of the static fracture displaying a crossover behavior that can be used as a sign of imminent failure. On the other hand, the numerically estimated apparent exponent for LLS is not universal. For event time intervals, a universal power law exponent γ close to unity is found in accordance with linear viscoelastic FBMs. The γ-value is very close to that obtained in fracturing processes over a wide range of activity. Moreover, the occurrence of burst avalanches in time-dependent breakdown is of importance in its own right due to the applicability of burst sequences in vastly different theoretical studies of the damage-failure process.

REFERENCES

[1] Zapperi S., Ray P., Stanley H. E. and Vespignani A., *Phys. Rev. E*, **59** (1999) 5049; *Phys. Rev. Lett.*, **78** (1997) 1408; Andersen J. V., Sornette D. and Leung K.-T., *Phys. Rev. Lett.*, **78** (1997) 2140.

[2] Guarino A., Ciliberto S., Garcimartín A. and Scorretti R., *Eur. Phys. J. B*, **26** (2002) 141; Maes C., Van Moffaert A., Frederix H. and Strauven H., *Phys. Rev. B*, **57** (1998) 4987; Vespignani A., Petri A., Alippi A. and Paparo G., *Fractals*, **3** (1995) 839; Davidsen J., Stanchits S. and Dresen G., *Phys. Rev. Lett.*, **98** (2007) 125502; Saichev A. and Sornette D., *Phys. Rev. E*, **71** (2005) 016608; Salminen L. I., Tolvanen A. I. and Alava M. J., *Phys. Rev. Lett.*, **89** (2002) 185503; Weiss J., Grasso J. R. and Martin P., in *Proceedings of the 6th International Conference on AE/MS in Geological Structure and Materials 1996* (Trans Tech Publications, Clausthal-Zellerfeld) 1988, pp. 583–595.

[3] Guarino A., Garcimartín A. and Ciliberto S., *Eur. Phys. J. B*, **6** (1998) 13.

[4] Omori F., *Rep. Earthq. Invest. Comm.*, **2** (1894) 103 (in Japanese).

[5] Gutenberg M. and Richter C. F., *Bull. Seismol. Soc. Am.*, **34** (1944) 185.

[6] Hirata T., *J. Geophys. Res.*, **92** (1987) 6215.

[7] Nechad H., Helmstetter A., El Guerjouma R. and Sornette D., *Phys. Rev. Lett.*, **94** (2005) 045501.

[8] Saichev A. and Sornette D., *Phys. Rev. E.*, **71** (2005) 016608.

[9] Herrmann H. J. and Roux S. (Editors), *Statistical Models for the Fracture of Disordered Media* (North-Holland, Amsterdam) 1990; Bhattacharyya P. and Chakrabarti B. K. (Editors), *Modelling Critical and Catastrophic Phenomena in Geoscience* (Springer-Verlag, Heidelberg) 2006.

[10] Daniels H., *Proc. R. Soc. London, Ser. A*, **183** (1945) 405.

[11] Coleman B. D., *J. Appl. Phys.*, **29** (1958) 968.

[12] Hidalgo R. C., Kun F. and Herrmann H. J., *Phys. Rev. E*, **65** (2002) 032502; Kun F., Hidalgo R. C., Herrmann H. J. and Pál K. F., *Phys. Rev. E*, **67** (2003) 061802.

[13] Kun F., Moreno Y., Hidalgo R. C. and Herrmann H. J., *Europhys. Lett.*, **63** (2003) 347.

[14] Ciliberto S., Guarino A. and Scorretti R., *Physica D*, **158** (2001) 83; Politi A., Guarino A. and Scorretti R., *Phys. Rev. E*, **66** (2002) 026107.

[15] Delaplace A., Roux S. and Pijaudier-Cabot G., *J. Eng. Mech.*, **127** (2001) 646; Baxevanis Th., Dufour F. and Pijaudier-Cabot G., *Int. J. Fract.*, **141** (2006) 561; Roux S., Delaplace A. and Pijaudier-Cabot G., *Physica A*, **270** (1999) 35.

[16] Baxevanis Th. and Katsaounis Th., *Phys. Rev. E*, **75** (2007) 046104.

[17] Baxevanis Th. and Katsaounis Th., in preparation.

[18] McLean D., *Rep. Prog. Phys.*, **29** (1996) 1; Cannon W. R. and Langdon T. G., *J. Mater. Sci.*, **23** (1998) 20.

[19] Kloster M., Hansen A. and Hemmer P. C., *Phys. Rev. E*, **56** (1997) 2615.

[20] Pradhan S., Hansen A. and Hemmer P. C, *Phys. Rev. Lett.*, **9** (2005) 125501.

[21] Hidalgo R. C., Kun F. C. and Herrmann H. J., *Physica A*, **347** (2005) 402.